Chromophore Structure in an Inactive State of a Novel Photosensor Protein Opn5L1: Resonance Raman Evidence for the Formation of a Deprotonated Adduct at the 11th Carbon Atom

Misao Mizuno,[1] Keita Sato,[2] Takahiro Yamashita,[3] Kazumi Sakai,[3] Yasushi Imamoto,[3] Yumiko Yamano,[4] Akimori Wada,[5] Hideyo Ohuchi,[2] Yoshinori Shichida,[3,6] and Yasuhisa Mizutani[1]*

[1] Department of Chemistry, Graduate School of Science, Osaka University, 1-1 Machikaneyama, Toyonaka, Osaka 560-0043, Japan

[2] Department of Cytology and Histology, Graduate School of Medicine, Dentistry and Pharmaceutical Sciences, Okayama University, 2-5-1 Shikata-cho, Kita-ku, Okayama, Okayama 700-8558, Japan

[3] Department of Biophysics, Graduate School of Science, Kyoto University, Kyoto 606-8502, Japan

[4] Comprehensive Education and Research Center, Kobe Pharmaceutical University, Kobe 658-8558, Japan

[5] Laboratory of Organic Chemistry for Life Science, Kobe Pharmaceutical University, 4-19-1 Motoyamakita-cho, Higashinada, Kobe, Hyogo 658-8558, Japan

[6] Research Organization for Science and Technology, Ritsumeikan University, Shiga 525-8577, Japan

ABSTRACT

Opsins are photosensitive G protein-coupled receptor proteins and are classified into visual and nonvisual receptors. Opn5L1 is a nonvisual opsin that binds all-*trans* retinal as a chromophore. A unique feature of Opn5L1 is that the protein exhibits a photocyclic reaction upon photoexcitation. Determining the chromophore structures of intermediates in the photocycle is essential for understanding the functional mechanism of Opn5L1. A previous study revealed that a long-lived intermediate in the photocycle cannot activate the G protein and forms a covalent bond between the retinal chromophore and a nearby cysteine residue. However, the position of this covalent bond in the chromophore remains undetermined. Here, we report a resonance Raman study on isotopically-labeled samples in combination with density functional theory calculations and reveal that the 11th carbon atom of the chromophore of the intermediate forms a covalent linkage to the cysteine residue. Furthermore, vibrational assignments based on the isotopic substitutions and density functional theory calculations suggested that the Schiff base of the intermediate is deprotonated. The chromophore structure determined in the present study well explains the mechanism of the photocyclic reaction, which is crucial to the photobiological function of Opn5L1.

INTRODUCTION

Light is a key source of information for animals involved in a variety of physiological activities. Opsins are photosensitive G protein-coupled receptor proteins universally found in animals and function for both visual and nonvisual photoreception.[1-2] All opsins share common structural elements, including seven transmembrane helices and a retinal chromophore linked via a Schiff base to a lysine residue. Recent genomic data reveal that animals possess several types of opsin genes and these can be categorized into numerous classes according to their sequences. Under dark conditions, most opsins bind 11-*cis* retinal as an inverse agonist, and photoisomerization of 11-*cis* retinal to the agonist all-*trans* retinal results in activation of the opsin and subsequent coupling with G protein.

Opn5 is the most recently discovered nonvisual opsin present in the human and mouse genomes.[3] Diverse subgroups of Opn5 genes have been found in a variety of animals, from fish to primates.[4-5] Opn5m is the sole Opn5 found in mammals, while non-mammalian vertebrates contain the Opn5L1 and Opn5L2 subgroups in addition to Opn5m. Opn5m and Opn5L2 bind 11-*cis* retinal to generate UV light-absorbing opsins.[6-10] UV light irradiation of Opn5m and Opn5L2 causes retinal isomerization to the all-*trans* form, resulting in a visible light-absorbing form active state. The visible light-absorbing forms are thermally stable and photoconvert back to the UV-absorbing form, and thus Opn5m and Opn5L2 exhibit photochromism. Examination of the ability to activate G protein showed that the UV-absorbing form is inactive and the visible light-absorbing form is active. Non-mammalian vertebrate Opn5m and Opn5L2 directly bind 11-*cis* and all-*trans* retinal to produce UV- and visible light-absorbing forms, respectively, whereas mammalian Opn5 incorporates exclusively 11-*cis* retinal to produce the UV-absorbing form. By contrast, Opn5L1 exclusively binds all-*trans* retinal and shows no photochromism. Instead,

visible photoexcitation leads to photoisomerization from the all-*trans* to the 11-*cis* form, followed by thermal reisomerization to form the original state with a time constant of about 3 h at 37 °C.[11] Opn5L1 is therefore characterized as a photocyclic opsin. The protein becomes inactive upon light illumination whereas the all-*trans* retinal-bound form is active.

Most notably, Opn5L1 generates a long-lived inactive intermediate showing an absorption band at 270 nm.[11] This 270-nm absorbing form has unique properties. High performance liquid chromatography (HPLC) analysis of an extract from the protein using hydroxylamine and organic solvent showed that no retinal isomers were extracted from the irradiated sample. Furthermore, absorption at the anomalously short wavelength of 270-nm of this absorbing form suggested that π conjugation in the polyene chain of the chromophore is broken. These experimental findings were explained by the formation of an adduct of the retinal chromophore with a nearby residue, Cys188. However, the position of this adduct in the retinal chromophore remains to be determined, although it was proposed that the thiol group of Cys188 reacts with the 11th carbon atom in the chromophore.[11] The protonation state of the Schiff base also remains to be clarified for the 270-nm absorbing form. The maximum absorption wavelengths[6, 8] suggest that the Schiff base in the UV-absorbing form is deprotonated for Opn5m and Opn5L2 but protonated in the visible light-absorbing form, implying that interconversion between the active and inactive forms accompanies the change in protonation state of the Schiff base for Opn5m and Opn5L2. It is therefore essential to determine the chromophore structure of the 270-nm absorbing form in terms of the position of adduct formation and the protonation state. Resonance Raman spectroscopy has made a significant contribution to the structural determination of the retinal chromophore of retinal proteins[12-13] and to understanding the photoreactions of chromophore model compounds.[14] The configurations[15-19] and distortion[20-25] of the polyene chain,

the protonation state of the Schiff base,[26] and the delocalization of the π electrons[27-28] were previously discussed for animal and microbial rhodopsins.

In the present study, we determined the chromophore structure of the 270-nm absorbing form of Opn5L1 using resonance Raman spectroscopy. Comparison of resonance Raman spectra containing isotopically-labeled chromophores showed that adduct formation involves Cys188 and the 11th carbon atom of the retinal. Furthermore, the results of vibrational assignments using isotopically-labeled samples in combination with density functional theory (DFT) calculations suggested that the Schiff base of the 270-nm absorbing form is deprotonated. The functional role of the structural features of the chromophore in the 270-nm absorbing form is discussed.

MATERIALS AND METHODS

Protein and Lipid Sample Preparation. The N- and C-termini of cDNA of chicken Opn5L1 were replaced by the corresponding termini from *Xenopus tropicalis* Opn5m to improve recombinant expression yield,[11] then the C-terminus was tagged with the Rho1D4 epitope sequence (ETSQVAPA) and inserted into the mammalian expression vector pCAGGS.[29] The plasmid DNA was transfected into HEK293T cells by the calcium phosphate method. Unlabeled (Sigma-Aldrich, R2500-500MG) or ^{13}C-labeled all-*trans*-retinal synthesized in-house was supplied to the culture medium at a final concentration of 5 μM. The cells were collected under dim red light 48 h after transfection. The proteins were extracted with 1% dodecyl maltoside (DM) in buffer A (50 mM HEPES (pH 7.0), 140 mM NaCl and 3 mM $MgCl_2$) and applied to Rho1D4 antibody-conjugated Sepharose beads. The purified Opn5L1 was eluted with buffer B (50 mM HEPES (pH 7.0), 20 mM NaCl and 3 mM $MgCl_2$) containing 0.02% DM and 0.45 mg/mL synthetic peptide with the Rho1D4 epitope sequence. The concentration of NaCl was

adjusted to 140 mM by the addition of 5 M NaCl after elution. The purified Opn5L1 was concentrated to between 8.7-16.7 μM using an Amicon Ultra-4 Centrifugal Filter Unit (Merck).

Cell lipids were extracted from HEK293T cells by phase-separation with methanol and chloroform. First, the HEK293T cells were collected and suspended in buffer A, then vigorously mixed with 2.5 volumes of methanol and 1.25 volumes of chloroform. After incubation at room temperature for 10 min, the mixture was vortexed after the addition of 1.25 volume of chloroform, vortexed again after the addition of 1.25 volume of buffer A, followed by centrifugation to separate the phases. The lower phases containing the cell lipids were collected and dried under an air stream. Finally, the cell lipids were resuspended in buffer A containing 0.02% DM.

Synthesis of Isotopically-Labeled Retinal and Dihydroretinal. 9-^{13}C-, 10-^{13}C-, 12-^{13}C- and 13-^{13}C-retinals were prepared according to a reported method.[30] 11,12-Dihydroretinal and its 13-^{13}C-labeled equivalent were synthesized from β-ionylideneacetoaldehyde.[31] Aldol condensation of β-ionylideneacetoaldehyde with C2-^{13}C acetone in toluene using sodium methoxide as the catalyst gave the ^{13}C-labeled C18-ketone. 1,4-Reduction of the C18-ketone using $Et(Me)_2SiH$[32] afforded ^{13}C-labeled dihydro-C18 ketone and subsequent Emmons-Horner-Wadsworth reaction with C2-cyanophosphonate generated ^{13}C-labeled dihydroretinonitrile. Finally, DIBAL reduction of the nitrile gave 13-^{13}C-11,12-dihydroretinal. Pure *E*-form was obtained by HPLC separation in the dark. Unlabeled 11,12-dihydroretinal was produced from unlabeled C18-ketone by the same procedures described above. Details of the synthetic procedures are described in the Supporting Information.

Dried 11,12-dihydroretinal in a glass test tube was dissolved and mixed with butylamine, then the solvent was evaporated under a nitrogen gas flow. This dissolution and evaporation

procedure was repeated once. The resultant 11,12-dihydroretinal Schiff base with butylamine was dissolved in methanol or 2.5% HCl-methanol to produce the deprotonated and protonated Schiff base samples, respectively.

Resonance Raman Measurements. The light source for the resonance Raman measurements was a Ti-sapphire laser pumped by a Q-switched LD-pumped Nd:YLF laser (Photonics Industries, TU-L) operating at 1 kHz. The fourth harmonic of the laser output, 238 nm, was used as the probe light. The typical power value of the probe light was 0.5 mW at the sample point. The probe pulse was focused into a line shape on the sample solution in a spinning cell using a cylindrical lens. The Raman scattering light was collected and focused onto the entrance slit of a Czerny-Turner configured Littrow prism prefilter (Bunkoukeiki, PF-200MP) coupled to a single spectrograph with a focal length of 550 mm (HORIBA Jobin Yvon, iHR550) by two achromatic doublet lenses. The dispersed light was detected with a liquid nitrogen-cooled CCD camera (Roper Scientific, SPEC-10:400B/LN-SN-U). The Raman shifts were calibrated using the Raman bands of cyclohexane and 2-propanol. The spectral dispersion was about 1 cm^{-1}/pixel on the CCD camera. The accumulation times were 60 min to obtain spectra of the protein, 30 min for the cell lipids, and 20 min for Trp and Tyr. The protein in the unphotolyzed state was converted to the 270-nm absorbing form by irradiating with yellow light (>500 nm) for resonance Raman measurements of the 270-nm absorbing form.

Quantum Chemical Calculations. The frequencies and Raman intensities of the vibrational modes for the model compounds were obtained by DFT calculations. Geometry optimization and normal mode analysis were performed at the B3LYP/6-311G(d,p) level. All calculations were conducted with the Gaussian 16W package.[33] The calculated frequencies were scaled using the wavenumber-linear scaling method.[34]

RESULTS

Resonance Raman Spectra in the 270-nm Absorbing Form of Opn5L1. Trace a in Figure 1 shows the resonance Raman spectrum of the wild type (WT) Opn5L1 sample after 3 min light irradiation to convert the protein to the 270-nm absorbing form. Traces b-d are the resonance Raman spectra of Tyr and Trp dissolved in buffer, and of the cell lipids solubilized with detergent in the buffer, respectively. Comparison of the spectra suggests that trace a predominantly contains spectral contributions from the cell lipids, which were not removed by the protein purification steps, and from Tyr and Trp residues. The Raman bands due to the chromophore of the 270-nm absorbing form were not apparent in trace a, although resonance enhancements of these bands were anticipated using a probe light of 238 nm.

We next compared the resonance Raman spectra of WT and the C188T mutant of Opn5L1 to identify the Raman bands of the chromophore. The spectral contributions of the chromophore of the 270-nm absorbing form should be revealed in the difference spectra between WT and the C188T mutant because the mutant is not photoconverted to the 270-nm absorbing form.[11] Trace a in Figure 2 shows the Raman spectra of WT and the C188T mutant after subtracting the spectral contributions of the cell lipids. The band intensities were normalized with respect to the peak of the Trp band at 1555 cm^{-1}. Trace b in Figure 2 shows the difference spectrum of WT and the C188T mutant. The prominent positive band at 1650 cm^{-1} with a shoulder at 1635 cm^{-1} is the spectral contribution of the chromophore of the 270-nm absorbing form. This band and shoulder are assignable to the C=C stretching modes because such bands are generally observed to be most intense in the resonance Raman spectra of polyenes. The C=C stretching frequency correlates with the length of the polyene chain. The observed frequency of 1650 cm^{-1} is consistent with the shortened polyene chain of the 270-nm absorbing form upon adduct

formation with Cys188. No remarkable bands in trace b were observed in the region below 1600 cm^{-1}, indicating the absence of spectral changes of the Trp and Tyr bands in the C188T mutant compared to WT.

We measured the resonance Raman spectra of WT Opn5L1 containing an isotopically-labeled retinal chromophore to allow vibrational assignment of the Raman bands around 1650 cm^{-1}. Figure 3 compares the Raman bands of the 270-nm absorbing form for Opn5L1 samples containing the unlabeled and ^{13}C-labeled chromophore. Trace a is a Raman spectrum of the unlabeled chromophore, and traces b–e are spectra of the chromophore ^{13}C-labeled at the 9th, 10th, 12th, and 13th positions (9-^{13}C, 10-^{13}C, 12-^{13}C, and 13-^{13}C), respectively. The spectral changes due to the isotopic substitutions corroborate the assignment that the bands are due to the Opn5L1 chromophore. The 1635 cm^{-1} band for the unlabeled chromophore downshifted to 1612 and 1624 cm^{-1} in the spectra of the 9-^{13}C- and 10-^{13}C-labeled chromophore, respectively, whereas the 9-^{13}C and 10-^{13}C substitutions had little effect on the position of the 1650 cm^{-1} band. The 12-^{13}C-labeled chromophore showed no noticeable downshift for the 1635 and 1650 cm^{-1} bands. A single band was observed at 1639 cm^{-1} in the spectrum of the 13-^{13}C-labeled chromophore, suggesting that the 1650 cm^{-1} band downshifted and overlapped with the 1635 cm^{-1} band. The observed isotope shifts showed that the 1635 and 1650 cm^{-1} bands were mainly due to the stretching modes of the C_9=C_{10} and the C_{13}=C_{14} bonds of the 270-nm absorbing form.

It should be noted that the 12-^{13}C-labeled chromophore showed no noticeable isotope shift. This result indicates that the 12th carbon does not form a double bond in the 270-nm absorbing form and that the thiol side chain of Cys188 forms the adduct at the 11th or 12th carbon. The retinal chromophore with a protonated Schiff base has a positive charge at the nitrogen atom or carbon atoms at odd-numbered positions in resonance structures, as shown in Figure S1 in the

Supporting Information. Positively charged atoms are more reactive in the nucleophilic addition reaction involving Cys188. Taken together, the observed isotope shifts provide strong experimental evidence that the thiol group in Cys188 forms a linkage to the carbon atom at the 11th position in the chromophore of Opn5L1, as proposed in our previous study.[11]

DFT Calculations of the Vibrational Spectra of the Chromophore in the 270-nm Absorbing Form of Opn5L1. We conducted DFT calculations for model compounds of the chromophore in the 270-nm form of Opn5L1 to verify the above-described vibrational assignments for the 1635 and 1650 cm^{-1} bands. Panels A and B in Figure 4 respectively show the protonated and deprotonated model compounds, and panels C and D show expanded views of the calculated spectra in the C=C stretching region for the unlabeled protonated and deprotonated forms, respectively. The calculated frequencies and intensities for the five bands are shown as black bars in each spectrum. Expanded views of the black traces are depicted in Figure S2 in the Supporting Information to show the presence of weak bands. Solid colored curves represent putative spectra obtained from the calculated frequencies and intensities of Gaussian bands with 20 cm^{-1} Gaussian full widths. The full width of 20 cm^{-1} was adopted since the band widths of Trp in buffer (trace c in Figure 1) were about 20 cm^{-1}. The calculated spectra for the isotopically-labeled model compounds are shown in panels E and F in Figure 4. The calculated frequencies for the unlabeled and labeled compounds are summarized in Table S1 in the Supporting Information. Optimized structures of the protonated and deprotonated model compounds are shown in Figure S3 in the Supporting Information.

Next, we focused on the stretching frequencies of the C=C bonds containing isotopically-labeled carbon atoms at the 9th, 10th or 13th positions. In the calculated spectra for the protonated form, the 1626 cm^{-1} band was ascribed to the C_9=C_{10} stretching mode since it

downshifted to 1603 cm^{-1} for both the 9-^{13}C- and 10-^{13}C-labeled chromophore. The lowest band at 1598 cm^{-1} for the unlabeled chromophore was assigned to the C_{13}=C_{14} stretching mode and downshifted to 1576 cm^{-1} upon isotopic labeling of the 13th carbon atom. The band at 1621 cm^{-1} showed no frequency change upon isotopic substitution and was ascribed to the in-phase combination of the C_5=C_6 and the C_7=C_8 stretching modes. The bands at 1646 and 1650 cm^{-1}, which are attributed to the out-of-phase combination of the C_5=C_6 and C_7=C_8 stretching modes, and the C_{15}=N stretching mode, respectively, showed isotope shifts of less than 2 cm^{-1}. Importantly, the calculated isotope shifts for the bands at 1646 and 1650 cm^{-1} contradict the experimental result that the 1650 cm^{-1} band exhibits a remarkable isotope shift upon 13-^{13}C labeling.

The DFT-calculated spectra for the deprotonated form showed that the bands at 1638 and 1653 cm^{-1} shifted to 1615/1613 and 1648/1650 cm^{-1}, respectively, upon isotopic labeling at the 9th/10th positions. These isotope shifts indicate that the bands have vibrational characters of the C_5=C_6 and C_9=C_{10} stretching modes. The 1652 and 1673 cm^{-1} bands were shown to contain the vibrational character of the C_{13}=C_{14} stretching mode. Notably, the band at 1673 cm^{-1} downshifted upon 13-^{13}C labeling, supporting the experimental result that the highest band downshifted for the 13-^{13}C-labeled chromophore. Thus, the isotope shifts of the calculated spectra for the deprotonated model compound were more similar to those of the observed spectra than were the calculated spectra for the protonated compound. The observed difference in the relative intensities of the double bands between the calculated and observed profiles is likely because the present calculations did not take into account the resonance Raman effect on band intensity.

Overall trends of the isotope frequency effect on the observed spectral profile were compared with the calculated profiles for the protonated and deprotonated forms. Panel G in Figure 4 compares the isotope effects on band positions with higher and lower frequencies between the experimental and calculated spectra. Two peak positions in the calculated spectra of both the protonated and deprotonated forms were determined by intensity-weighted averages of the calculated frequencies for the modes comprising the higher and lower bands. In the experimental spectra, a downshift of the higher frequency band was observed only for the 13-^{13}C derivative whereas a downshift of the lower frequency band was observed for the 9-^{13}C and 10-^{13}C derivatives. These features were reproduced in the calculated spectra for the deprotonated forms. Absolute vibrational frequencies provided by DFT calculations can show deviations from experimentally observed frequencies but the calculations provide more accurate values for isotope frequency shifts. Accordingly, comparison of the experimental and calculated isotope frequency shifts suggests that the chromophore of the 270-nm absorbing form of Opn5L1 is deprotonated.

Resonance Raman Spectra of a Model Compound of the Chromophore. Resonance Raman spectra of a synthetic model compound of the 11,12-dihydro chromophore, 11,12-dihydroretinal Schiff base with butylamine, were measured for the protonated and deprotonated forms to verify the hypothesis that the chromophore of the 270-nm absorbing form of Opn5L1 is deprotonated. The excitation wavelength of 238 nm for obtaining the Raman spectra was resonant with the electronic transitions of the protonated and deprotonated model compounds with absorption maxima of 270 and 240 nm, respectively.[35] The red traces in Figure 5A and 5B show expanded views of the C=C stretching regions of the resonance Raman spectra of the protonated and deprotonated model compounds, the spectra of the 13-^{13}C derivatives of the

model compounds are shown in blue, and the black traces represent difference spectra between the unlabeled model compound and its 13-^{13}C derivative in the protonated and deprotonated forms, respectively.

Bands at 1628, 1642, and 1677 cm^{-1} were observed for the unlabeled model compound in the protonated form (Figure 5A). The band at 1628 cm^{-1} shifted to 1604 cm^{-1} upon isotopic substitution. For the deprotonated form (Figure 5B), a strong band at 1656 cm^{-1} was observed with a weak shoulder at 1619 cm^{-1} for the unlabeled model, and the band at 1656 cm^{-1} shifted to 1642 cm^{-1} upon isotopic substitution. A difference spectrum between the unlabeled and 13-^{13}C-labeled chromophore in Opn5L1 is shown in Figure 5C, which is similar to the difference spectrum for the deprotonated model compound. Furthermore, the DFT-calculated frequencies for the deprotonated form were consistent with the experimental observation that isotopic substitution at the 13th position resulted in a downshift of the higher frequency band. Accordingly, the resonance Raman spectra and the DFT calculations for the model compounds consistently demonstrate that the chromophore of the 270-nm absorbing species of Opn5L1 is deprotonated.

DISCUSSION

The present study provided experimental and computational evidence that the 270-nm absorbing form of the Opn5L1 chromophore forms a covalent linkage at the 11th carbon atom and has a deprotonated Schiff base. It is likely after adduct formation that the Schiff base releases a proton, since the delocalized positive charge on the polyene chain in the protonated form facilitates the nucleophilic attack of Cys188. The structural changes proposed in the present study are depicted in Figure 6.

Determination of the Position for Adduct Formation between the Retinal Chromophore and Cys188. Our previous report provided a model of Opn5L1 function, in which the retinal chromophore of Opn5L1 forms an adduct at the 11th carbon atom to Cys188 following photoexcitation.[11] The present study established that the adduct is formed at the 11th carbon atom. Adduct formation results in conversion of the C_{11}=C_{12} double bond to a single bond and can thus assist thermal recovery to the unphotolyzed state. A role of the residue at position 188, which is close to the 11th carbon of the chromophore in the photoreaction of rhodopsins, was previously discussed based on the model.[11] The T188C mutant of Opn5m exclusively bound all-*trans* retinal and thermally self-regenerated to the original form after photoexcitation, which is similar to the properties of Opn5L1.[36] The G188C mutant of bovine rhodopsin exhibited accelerated thermal recovery to the unphotolyzed state.[37] A possible mechanism for this acceleration is that the cysteine residue introduced at position 188 transiently forms an adduct with the all-*trans* retinal chromophore after photoactivation and quickly dissociates from the retinal chromophore after isomerization to 11-*cis* retinal. The determination of the position for adduct formation in the present study will thus help in understanding the roles of the residue at position 188 in rhodopsins.

Possible Functional Roles of Deprotonation in the Retinal Chromophore of Opn5L1. The shorter the π conjugation of the retinal chromophore, the lower the pK_a of the Schiff base because less delocalization of the positive charge destabilizes the protonated form. It is therefore likely that the formation of an adduct with Cys188 facilitates deprotonation at the Schiff base.

A possible role of deprotonation is that it stabilizes the 270-nm absorbing form in the photocycle. Conversion of the C_{11}=C_{12} bond to a single bond is advantageous because it facilities thermal reisomerization from the 11-*cis* form to the all-*trans* form. However, this facilitation is

not possible if the Cys188-bound 11-*cis* chromophore is converted back to the Cys188-unbound 11-*cis* form. The delocalized positive charge in the protonated chromophore can promote water-catalyzed dissociation of Cys188 from the chromophore: i.e., a back-reaction. Deprotonation in the 270-nm absorbing form can prevent this back-reaction by making the π electrons less delocalized in the chromophore of Opn5L1.

CONCLUSION

Resonance Raman spectra of the isotopically-labeled chromophore in the 270-nm absorbing form of Opn5L1 provided structural information regarding the position of adduct formation with the cysteine residue and on the protonation state of the Schiff base. The present observations on the C=C stretching frequencies determined that the chromophore structure of the 270-nm absorbing form arises when the Cys188 residue covalently links to the carbon atom at the 11th position and the Schiff base is deprotonated. Our determination that adduct formation occurs at the 11th carbon atom helps in understanding the roles of the residue at position 188 in rhodopsins. Deprotonation at the Schiff base can lengthen the lifetime of the 270-nm absorbing form, which serves as the inactive state for G-protein activation in the photocycle of Opn5L1.

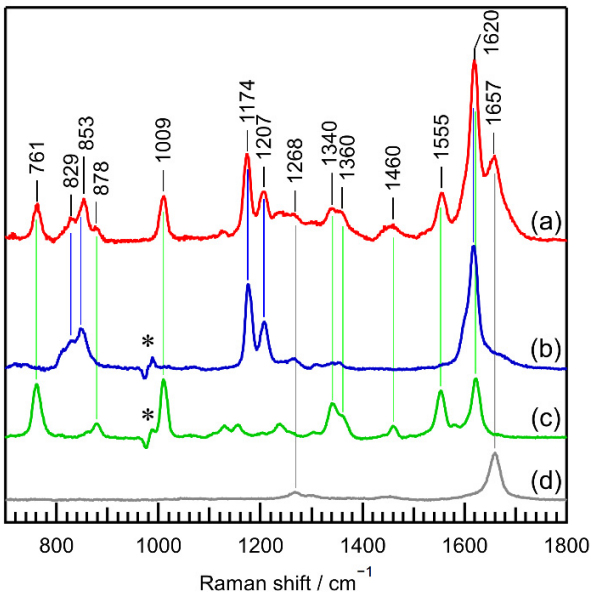

Figure 1. Resonance Raman spectra of (a) WT Opn5L1, (b) Tyr, (c) Trp, and (d) cell lipids excited at 238 nm. The spectrum of Opn5L1 was obtained after 3 min irradiation with > 500 nm light. The spectrum of the buffer has been subtracted in each spectrum. The asterisks represent the band due to sulfate ion in the buffer for the Tyr and Trp solutions.

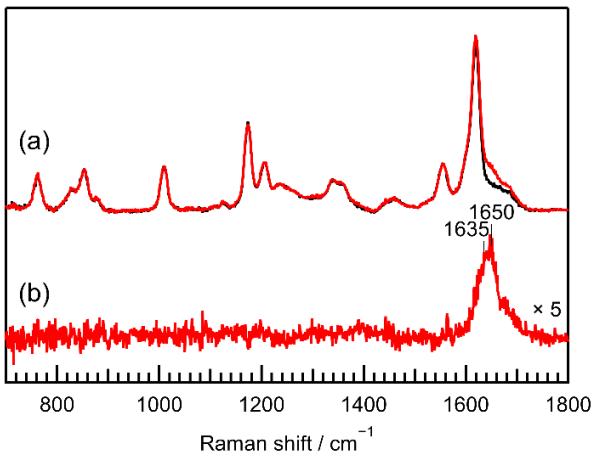

Figure 2. Resonance Raman spectra of Opn5L1 excited at 238 nm. (a) Spectra of WT (red) and the C188T mutant (black) of Opn5L1. The spectra were obtained after 3 min irradiation with > 500 nm light. Spectral contributions of the buffer and the lipid in the sample have been subtracted. The intensity was normalized using the tryptophan band at 1555 cm^{-1}. (b) The difference spectrum between WT and the C188T mutant, representing the resonance Raman spectrum of the 270-nm absorbing species. The band intensity is magnified by a factor of 5.

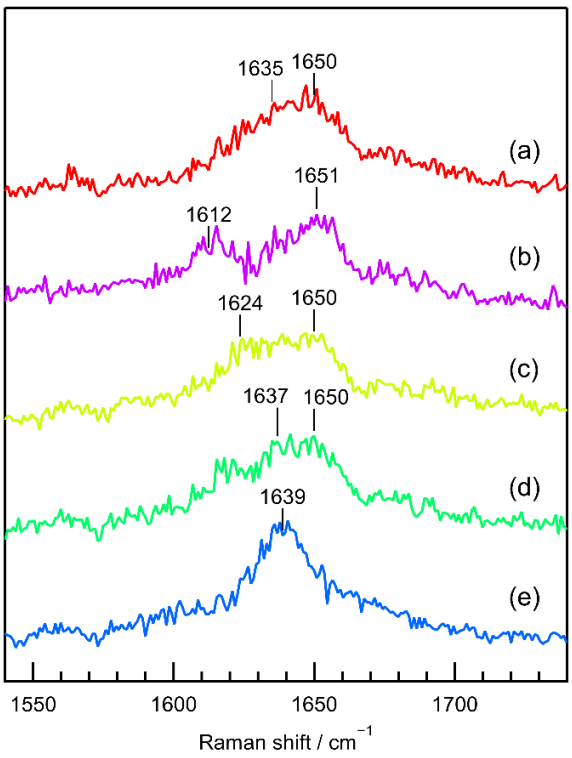

Figure 3. Expanded views of the difference Raman spectra of the 270-nm absorbing species of Opn5L1. (a) Unlabeled chromophore and (b) 9-^{13}C-, (c) 10-^{13}C-, (d) 12-^{13}C-, and (e) 13-^{13}C-labeled chromophore in the 270-nm absorbing species.

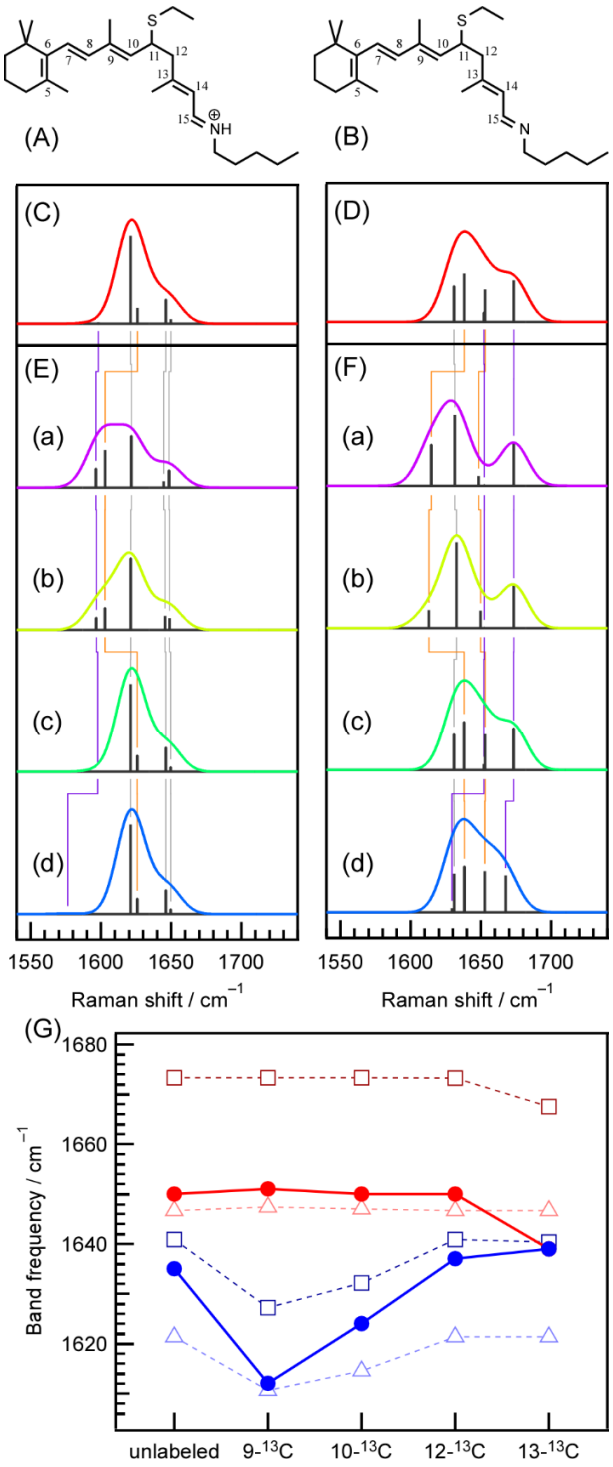

Figure 4. Calculated spectra of the model compounds of the 270-nm absorbing species of Opn5L1. (A and B) Structures of (A) the protonated and (B) deprotonated forms of the model compound. (C–F) Calculated spectra of the C=C stretching bands. Panels C and E are the

calculated spectra of the protonated forms of the unlabeled and isotopically-labeled derivatives, respectively. Panels D and F are the calculated spectra of the deprotonated forms of the unlabeled and isotopically-labeled derivatives, respectively. Traces a–d in panels E and F are the spectra of the 9-^{13}C, 10-^{13}C, 12-^{13}C, and 13-^{13}C derivatives, respectively. Black bars represent the calculated spectra. Colored traces show the sum of the bands represented by a Gaussian function with a full Gaussian bandwidth of 20 cm^{-1}. Orange, purple, and gray connectors indicate the isotope shifts of the bands due to double bond stretching modes at the C_9=C_{10}, C_{13}=C_{14}, and other (C_5=C_6, C_7=C_8, and C_{15}=N) bonds, respectively. Normal modes of the bands are described in Table S1 in the Supporting Information. (G) Isotope effects on the apparent band frequencies. Red- and blue-colored symbols are the frequencies of the two observed bands appearing at higher and lower frequencies, respectively. Closed circles represent the frequencies of the two bands observed in the experimental spectra, and the open triangles and open squares those in the calculated spectra of the protonated and deprotonated forms. The frequencies in the calculated spectra were determined as intensity-weighted averages of the calculated frequencies for the modes comprising the higher and lower bands. For the protonated form, the higher and lower frequencies are the intensity-weighted averages for higher two and lower three modes, respectively. For the deprotonated form, the higher and lower frequencies are one of the highest mode and the intensity-weighted averages for lower four modes, respectively.

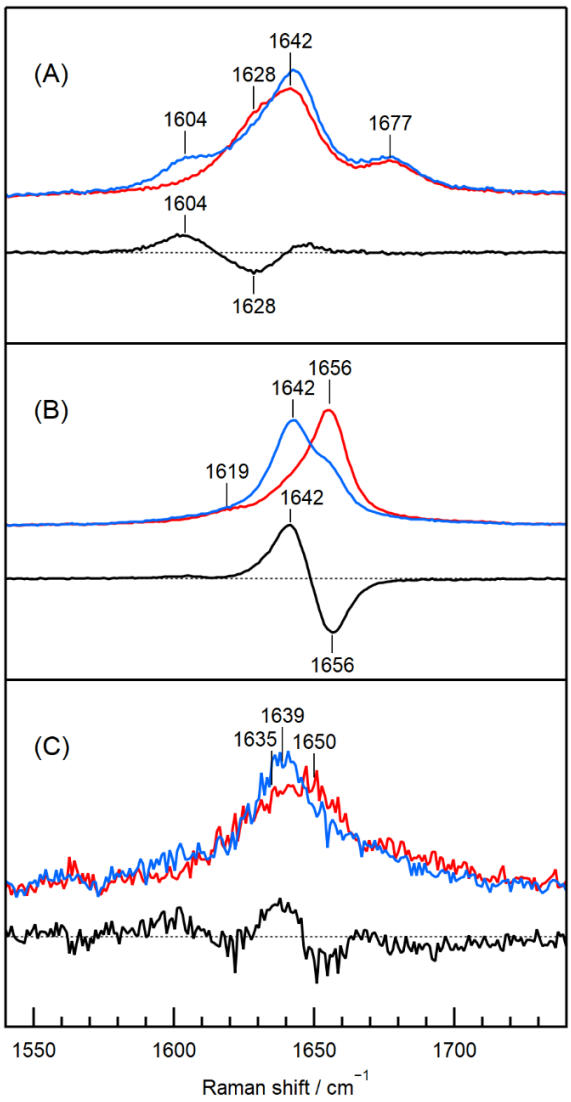

Figure 5. Resonance Raman spectra of the 11,12-dihydroretinal Schiff base with butylamine in (A) the protonated and (B) deprotonated forms in methanol. The excitation wavelength was 238 nm. For each panel, red and blue traces represent the spectrum of the unlabeled and 13-^{13}C-labeled derivatives. The black trace is the difference spectrum between the unlabeled and labeled spectra. (C) Resonance Raman spectra of the unlabeled (red) and 13-^{13}C-labeled chromophore (blue) in the in the 270-nm absorbing species and their difference spectrum (black).

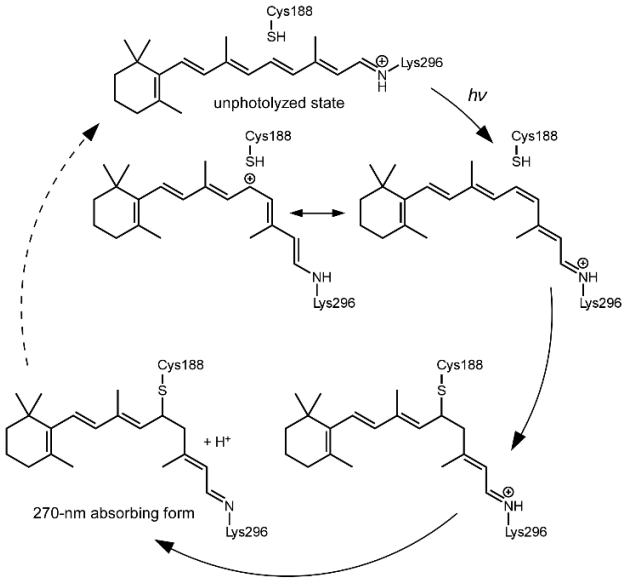

Figure 6. Proposed structural changes of the retinal chromophore in the photocycle of Opn5L1.

ASSOCIATED CONTENT

Supporting Information.

The following files are available free of charge.

Synthesis of isotopically-labeled retinal and dihydroretinal, resonance structures of the protonated form of 11-*cis* retinal chromophore, expanded views of the DFT-calculated spectra of the C=C stretching bands, vibrational assignments of the C=C stretching modes, and optimized structures of the protonated and deprotonated model compounds for the DFT calculations (PDF)

AUTHOR INFORMATION

Corresponding Author

Yasuhisa Mizutani — *Department of Chemistry, Graduate School of Science, Osaka University, 1-1 Machikaneyama, Toyonaka, Osaka 560-0043, Japan*; orcid.org/0000-0002-3754-5720; Email: mztn@chem.sci.osaka-u.ac.jp; Phone: +81-6-6850-5776.

Notes

The authors declare no competing financial interest.

ACKNOWLEDGMENT

The authors thank Prof. R.S. Molday for the generous gift of a Rho1D4-producing hybridoma. This work was supported by MEXT KAKENHI Grant Number JP25104006 to YM, JSPS KAKENHI Grant Number JP20K08885 to KS, JST-CREST Grant Number JPMJCR1753 to TY, and AMED-CREST Grant Number 22gm1510007 to TY.

REFERENCES

1. Shichida, Y.; Matsuyama, T., Evolution of Opsins and Phototransduction. *Philos. Trans. R. Soc. B* **2009,** *364*, 2881-2895.
2. Koyanagi, M.; Terakita, A., Diversity of Animal Opsin-Based Pigments and Their Optogenetic Potential. *Biochim. Biophys. Acta* **2014,** *1837*, 710-716.
3. Tarttelin, E. E.; Bellingham, J.; Hankins, M. W.; Foster, R. G.; Lucas, R. J., Neuropsin (Opn5): A Novel Opsin Identified in Mammalian Neural Tissue. *FEBS Lett.* **2003,** *554*, 410-416.
4. Tomonari, S.; Migita, K.; Takagi, A.; Noji, S.; Ohuchi, H., Expression Patterns of the Opsin 5–Related Genes in the Developing Chicken Retina. *Dev. Dyn.* **2008,** *237*, 1910-1922.
5. Yamashita, T., Unexpected Molecular Diversity of Vertebrate Nonvisual Opsin Opn5. *Biophys. Rev.* **2020,** *12*, 333-338.
6. Yamashita, T.; Ohuchi, H.; Tomonari, S.; Ikeda, K.; Sakai, K.; Shichida, Y., Opn5 Is a UV-Sensitive Bistable Pigment That Couples with Gi Subtype of G Protein. *Proc. Natl. Acad. Sci. USA* **2010,** *107*, 22084-22089.
7. Kojima, D.; Mori, S.; Torii, M.; Wada, A.; Morishita, R.; Fukada, Y., UV-Sensitive Photoreceptor Protein Opn5 in Humans and Mice. *PLOS ONE* **2011,** *6*, e26388.
8. Ohuchi, H.; Yamashita, T.; Tomonari, S.; Fujita-Yanagibayashi, S.; Sakai, K.; Noji, S.; Shichida, Y., A Non-Mammalian Type Opsin 5 Functions Dually in the Photoreceptive and Non-Photoreceptive Organs of Birds. *PLOS ONE* **2012,** *7*, e31534.
9. Yamashita, T.; Ono, K.; Ohuchi, H.; Yumoto, A.; Gotoh, H.; Tomonari, S.; Sakai, K.; Fujita, H.; Imamoto, Y.; Noji, S., et al., Evolution of Mammalian Opn5 as a Specialized UV-Absorbing Pigment by a Single Amino Acid Mutation. *J. Biol. Chem.* **2014,** *289*, 3991-4000.
10. Sato, K.; Yamashita, T.; Haruki, Y.; Ohuchi, H.; Kinoshita, M.; Shichida, Y., Two UV-Sensitive Photoreceptor Proteins, Opn5m and Opn5m2 in Ray-Finned Fish with Distinct Molecular Properties and Broad Distribution in the Retina and Brain. *PLOS ONE* **2016,** *11*, e0155339.
11. Sato, K.; Yamashita, T.; Ohuchi, H.; Takeuchi, A.; Gotoh, H.; Ono, K.; Mizuno, M.; Mizutani, Y.; Tomonari, S.; Sakai, K., et al., Opn5L1 Is a Retinal Receptor That Behaves as a Reverse and Self-Regenerating Photoreceptor. *Nat. Commun.* **2018,** *9*, 1255.
12. Mathies, R. A.; Smith, S. O.; Palings, I., Determination of Retinal Chromophore Structure in Rhodopsins. In *Biological Application of Raman Spectroscopy*, Spiro, T. G., Ed.; John Wiley and Sons: New York, 1988; Vol. II, pp 59-108.
13. Althaus, T.; Eisfeld, W.; Lohrmann, R.; Stockburger, M., Application of Raman Spectroscopy to Retinal Proteins. *Isr. J. Chem.* **1995,** *35*, 227-251.
14. Hamaguchi, H.-o.; Okamoto, H.; Tasumi, M.; Mukai, Y.; Koyama, Y., Transient Raman Spectra of the All-trans and 7-, 9-, 11- and 13-Mono-cis Isomers of Retinal and the Mechanism of the cis-trans Isomerization in the Lowest Excited Triplet State. *Chem. Phys. Lett.* **1984,** *107*, 355-359.
15. Mathies, R.; Freedman, T. B.; Stryer, L., Resonance Raman Studies of the Conformation of Retinal in Rhodopsin and Isorhodopsin. *J. Mol. Biol.* **1977,** *109*, 367-372.
16. Braiman, M.; Mathies, R., Resonance Raman Evidence for an All-Trans to 13-Cis Isomerization in the Proton-Pumping Cycle of Bacteriorhodopsin. *Biochemistry* **1980,** *19*, 5421-5428.
17. Palings, I.; Pardoen, J. A.; Van den Berg, E.; Winkel, C.; Lugtenburg, J.; Mathies, R. A., Assignment of Fingerprint Vibrations in the Resonance Raman Spectra of Rhodopsin,

Isorhodopsin, and Bathorhodopsin: Implications for Chromophore Structure and Environment. *Biochemistry* **1987,** *26*, 2544-2556.
18. Fodor, S. P.; Pollard, W. T.; Gebhard, R.; van den Berg, E. M.; Lugtenburg, J.; Mathies, R. A., Bacteriorhodopsin's L_{550} Intermediate Contains a C14-C15 S-*trans*-Retinal Chromophore. *Proc. Natl. Acad. Sci. USA* **1988,** *85*, 2156-2160.
19. Fodor, S. P. A.; Ames, J. B.; Gebhard, R.; van den Berg, E. M. M.; Stoeckenius, W.; Lugtenburg, J.; Mathies, R. A., Chromophore Structure in Bacteriorhodopsin's N Intermediate: Implications for the Proton-Pumping Mechanism. *Biochemistry* **1988,** *27*, 7097-7101.
20. Smith, S. O.; Pardoen, J. A.; Mulder, P. P. J.; Curry, B.; Lugtenburg, J.; Mathies, R., Chromophore Structure in Bacteriorhodopsin's O_{640} Photointermediate. *Biochemistry* **1983,** *22*, 6141-6148.
21. Smith, S. O.; Pardoen, J. A.; Lugtenburg, J.; Mathies, R. A., Vibrational Analysis of the 13-*cis*-Retinal Chromophore in Dark-Adapted Bacteriorhodopsin. *J. Phys. Chem.* **1987,** *91*, 804-819.
22. Smith, S. O.; Braiman, M. S.; Myers, A. B.; Pardoen, J. A.; Courtin, J. M. L.; Winkel, C.; Lugtenburg, J.; Mathies, R. A., Vibrational Analysis of the All-*trans*-Retinal Chromophore in Light-Adapted Bacteriorhodopsin. *J. Am. Chem. Soc.* **1987,** *109*, 3108-3125.
23. Palings, I.; Van den Berg, E. M. M.; Lugtenburg, J.; Mathies, R. A., Complete Assignment of the Hydrogen out-of-Plane Wagging Vibrations of Bathorhodopsin: Chromophore Structure and Energy Storage in the Primary Photoproduct of Vision. *Biochemistry* **1989,** *28*, 1498-1507.
24. Lohrmann, R.; Stockburger, M., Time-Resolved Resonance Raman Studies of Bacteriorhodopsin and Its Intermediates K590 and L550: Biological Implications. *J. Raman Spectrosc.* **1992,** *23*, 575-583.
25. Nishimura, N.; Mizuno, M.; Kandori, H.; Mizutani, Y., Distortion and a Strong Hydrogen Bond in the Retinal Chromophore Enable Sodium-Ion Transport by the Sodium-Ion Pump KR2. *J. Phys. Chem. B* **2019,** *123*, 3430-3440.
26. Baasov, T.; Friedman, N.; Sheves, M., Factors Affecting the C=N Stretching in Protonated Retinal Schiff Base: A Model Study for Bacteriorhodopsin and Visual Pigments. *Biochemistry* **1987,** *26*, 3210-3217.
27. Aton, B.; Doukas, A. G.; Callender, R. H.; Becher, B.; Ebrey, T. G., Resonance Raman Studies of the Purple Membrane. *Biochemistry* **1977,** *16*, 2995-2999.
28. Otomo, A.; Mizuno, M.; Singh, M.; Shihoya, W.; Inoue, K.; Nureki, O.; Béjà, O.; Kandori, H.; Mizutani, Y., Resonance Raman Investigation of the Chromophore Structure of Heliorhodopsins. *J. Phys. Chem. Lett.* **2018,** *9*, 6431-6436.
29. Niwa, H.; Yamamura, K.-i.; Miyazaki, J.-i., Efficient Selection for High-Expression Transfectants with a Novel Eukaryotic Vector. *Gene* **1991,** *108*, 193-199.
30. Lugtenburg, J., The Synthesis of ^{13}C-Labelled Retinals. *Pure Appl. Chem.* **1985,** *57*, 753-762.
31. Wada, A.; Fujioka, N.; Tanaka, Y.; Ito, M., A Highly Stereoselective Synthesis of 11*Z*-Retinal Using Tricarbonyliron Complex. *J. Org. Chem.* **2000,** *65*, 2438-2443.
32. Ojima, I.; Kogure, T., Reduction of Carbonyl Compounds Via Hydrosilylation. 4. Highly Regioselective Reductions of α, β-Unsaturated Carbonyl Compounds. *Organometallics* **1982,** *1*, 1390-1399.

33. Frisch, M. J.; Trucks, G. W.; Schlegel, H. B.; Scuseria, G. E.; Robb, M. A.; Cheeseman, J. R.; Scalmani, G.; Barone, V.; Petersson, G. A.; Nakatsuji, H., et al. *Gaussian 16 Rev. C.01*, Wallingford, CT, 2016.
34. Yoshida, H.; Ehara, A.; Matsuura, H., Density Functional Vibrational Analysis Using Wavenumber-Linear Scale Factors. *Chem. Phys. Lett.* **2000,** *325*, 477-483.
35. Gawinowicz, M. A.; Balogh-Nair, V.; Sabol, J. S.; Nakanishi, K., A Nonbleachable Rhodopsin Analogue Formed from 11,12-Dihydroretinal. *J. Am. Chem. Soc.* **1977,** *99*, 7720-7721.
36. Fujiyabu, C.; Sato, K.; Nishio, Y.; Imamoto, Y.; Ohuchi, H.; Shichida, Y.; Yamashita, T., Amino Acid Residue at Position 188 Determines the UV-Sensitive Bistable Property of Vertebrate Non-Visual Opsin Opn5. *Commun. Biol.* **2022,** *5*, 63.
37. Sakai, K.; Shichida, Y.; Imamoto, Y.; Yamashita, T., Creation of Photocyclic Vertebrate Rhodopsin by Single Amino Acid Substitution. *eLife* **2022,** *11*, e75979.

TOC graphic